ACS APPLIED MATERIALS & INTERFACES

Research Article

Cite This: ACS Appl. Mater. Interfaces 2018, 10, 3929–3937

www.acsami.org

Tailor-Making Fluorescent Hyaluronic Acid Microgels via Combining Microfluidics and Photoclick Chemistry for Sustained and Localized Delivery of Herceptin in Tumors

Jing Chen, Ke Huang, Qijun Chen, Chao Deng,* Jian Zhang, and Zhiyuan Zhong*

Biomedical Polymers Laboratory, and Jiangsu Key Laboratory of Advanced Functional Polymer Design and Application, College of Chemistry, Chemical Engineering and Materials Science, Soochow University, Suzhou 215123, People's Republic of China

Supporting Information

ABSTRACT: Antibody therapeutics, though representing a most used biomedicine, suffers from poor in vivo stability, rapid degradation, and frequent injections. Here, we report that fluorescent hyaluronic acid microgels (HMGs) tailor-made by combining microfluidics and "tetrazole−alkene" photoclick chemistry enable sustained and localized delivery of Herceptin in ovarian tumors. HMGs were obtained with a defined size (25−50 μm), narrow size distribution, high stability, and strong green fluorescence. Notably, HMGs exhibited a remarkably high loading of proteins such as Herceptin and IgG with a loading efficiency exceeding 90% at a theoretical protein-loading content of 30 wt %. In vitro protein release experiments revealed a sustained and hyaluronidase (HAase)-dependent release of Herceptin from HMGs, in which 80.6% of Herceptin was released at 1 U/mL HAase in 10 days. The released Herceptin maintained its secondary structure and antitumor activity. In vivo imaging results demonstrated obviously better tumoral retention for Cy5-labeled Herceptin-loaded HMGs following subcutaneous (sc) injection than for the free-protein counterpart. Interestingly, sc injection of the Herceptin-loaded HMGs into SKOV-3 human ovarian tumor-bearing nude mice at a dose of 30 mg Herceptin equiv/kg induced nearly complete tumor suppression, which was significantly more effective than the sc or systemic injection of free Herceptin. These tailor-made fluorescent HMGs appeared as a robust injectable platform for sustained and localized delivery of therapeutic proteins.

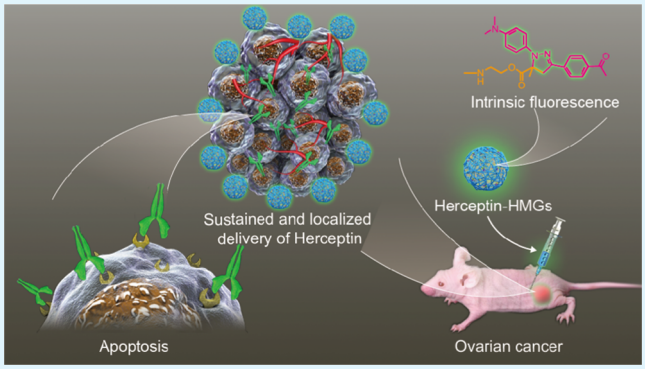

KEYWORDS: *microgels, microfluidics, click reaction, protein release, cancer therapy*

1. INTRODUCTION

Antibody therapeutics is a most used biomedicine that effectively treats various diseases including cancers.[1,2] Unlike chemical drugs, antibody therapeutics shows a notably high specificity. For example, Herceptin (trastuzumab), a recombinant monoclonal antibody specific for HER2-receptors, has been extensively employed to treat HER2-overexpressing metastatic breast cancer in clinics.[3] Benefited from its superb anticancer efficacy, Herceptin is currently being actively investigated for the treatment of other HER2-overexpressing cancers such as ovarian cancer and gastric carcinoma.[4−6] It should be noted, however, that antibody therapeutics including Herceptin often shows poor in vivo stability and tumoral retention and needs to be administered weekly via intravenous (iv) infusion.[7,8]

To improve patient compliance and enhance protein therapeutic effect, many different systems including microparticles, hydrogels, and microgels have been developed for the sustained local release of protein drugs.[9−14] For example, sustained protein releasing formulations such as LUPRON DEPOT, Suprecur MP, and Decapeptyl have been developed based on biodegradable poly(lactic-*co*-glycolic acid) (PLGA) microparticles for the treatment of prostate cancer in clinics.[15] The sustained and local delivery of immunomodulatory antibodies (anti-CD40 and anti-CTLA-4) using PLGA microparticles was reported to induce potent therapeutic efficacy in colon carcinoma-bearing mice.[16,17] However, the acidic degradation products of PLGA microparticles often cause denaturation of encapsulated proteins and local tissue inflammation.[18] Hydrogels with a high water content, excellent biocompatibility, and high protein-loading capacity have been extensively investigated for the local and sustained delivery of therapeutic proteins.[9,19] Injectable hydrogels facilitating protein encapsulation and noninvasive administration have attracted particular interest.[13] It is worthy to note, however, that injectable hydrogels are challenged with stringent requirements

Received: October 18, 2017
Accepted: January 5, 2018
Published: January 5, 2018

DOI: 10.1021/acsami.7b15832
ACS Appl. Mater. Interfaces 2018, 10, 3929–3937

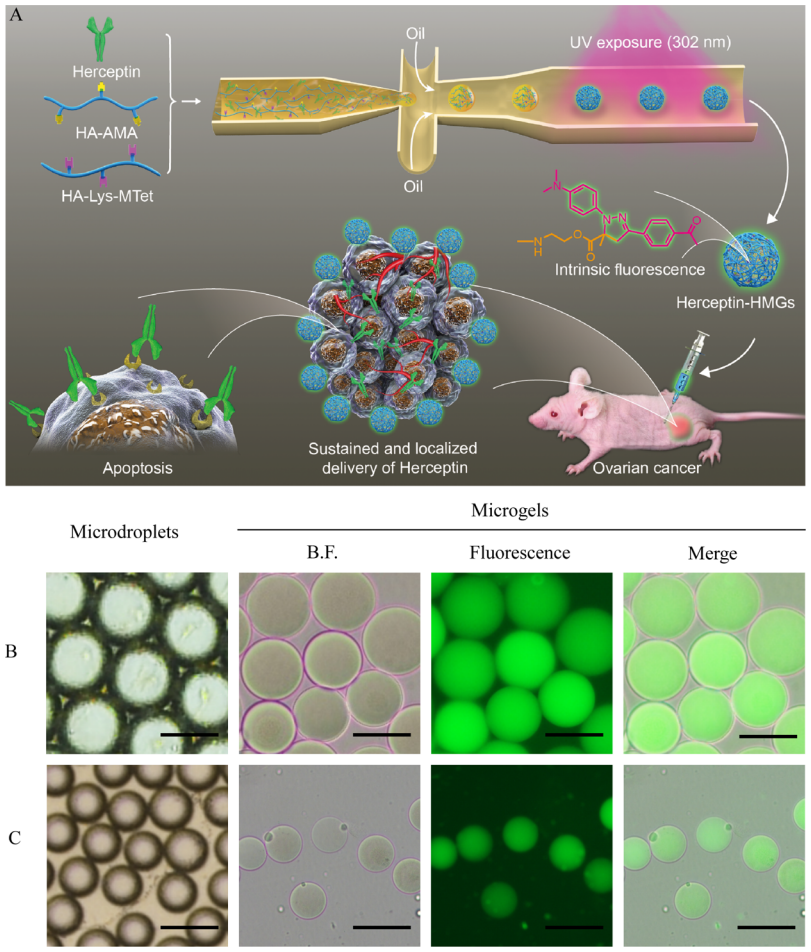

Figure 1. (A) Schematic illustration of fluorescent HMGs tailor-made by combining microfluidics and tetrazole−alkene photoclick chemistry for the sustained and localized delivery of Herceptin in ovarian tumor; (B,C) size and morphology of HA microdroplets and microgels (HMGs) visualized by fluorescence microscopy. Conditions: (B) Q_o = 5 μL/min and Q_w = 1 μL/min; (C) Q_o = 10 μL/min and Q_w = 1 μL/min. Scale bars, 50 μm.

on, for example, cross-linking methods and gelation time. In comparison, microgels uniquely combining the advantages of PLGA microparticles and hydrogels have appeared to be a most ideal system for local protein delivery. For example, peptide and polysaccharide microgels developed through desolvation or physical cross-linking with copper/calcium ions were shown to efficiently encapsulate proteins such as green fluorescent protein, wheat germ agglutinin, and bovine serum albumin, and the released proteins maintained their bioactivity.[20−22] However, these physically cross-linked microgels often exhibit burst protein release. Microgels developed through esterification of poly(acrylic acid) and poly(ethylene glycol) (PEG) were reported to accomplish a long-term release of lysozyme over 30 days.[23] Microgels formed by inverse emulsion polymerization or electrospray procedure and covalently decorated with glucose oxidase could facilitate insulin release leading to a reduction of blood glucose levels in a mouse model of type-I diabetes.[24,25] Recently, PEG microgels cross-linked with a protease-degradable peptide via a Michael-type addition reaction were shown to remain in the subcutaneous (sc) space of mice and promote in vivo vascularization by the sustained release of vascular endothelial growth factor.[26] It is interesting to note that no microgels have been developed for the local delivery of anticancer proteins.

Here, we report on novel fluorescent hyaluronic acid microgels (HMGs) tailor-made by combining microfluidics and "tetrazole−alkene" photoclick chemistry for the sustained and localized delivery of Herceptin in ovarian tumor in vivo (Figure 1A). The microfluidics technique allows precise control over the size of microgels.[26,27] The tetrazole−alkene photoclick reaction was catalyst-free and shown to have a high specificity and protein compatibility.[28,29] Hyaluronic acid (HA) is a biocompatible natural material prone to degradation with hyaluronidase (HAase),[30−32] which is abundant in the tumor microenvironment.[31] It should further be noted that these photoclick microgels possess a strong green fluorescence, as for photoclick hydrogels and nanogels,[29,33] which makes them easily traceable in the tumor.

2. EXPERIMENTAL SECTION

2.1. Synthesis of HA-*g*-AMA and HA-*g*-Lys-MTet. Hyaluronic acid-*g*-2-aminoethyl methacrylate (HA-*g*-AMA) was prepared through the amidation of HA and AMA in the presence of 4-(4,6-dimethoxy-1,3,5-triazin-2-yl)-4-methylmorpholinium chloride (DMTMM) (Scheme S1). Typically, HA (500 mg, 14.29 μmol) and AMA (47 mg, 286 μmol) were dissolved in deionized (DI) water (25 mL) under N_2, followed by adjusting the pH to 6.4−6.7. DMTMM (119 mg, 425 μmol) was added. The reaction proceeded at 35 °C for 24 h in the dark, and the product was isolated by extensive dialysis [a molecular weight cutoff (MWCO) of 3500] against DI water, followed by lyophilization. Yield: 90%. ^{1}H NMR (400 MHz, D_2O, Figure S1, δ): AMA: 1.86, 3.96, 4.17, 5.68, 6.08; HA: 1.96, 3.28−3.84, 4.41−4.47. The degree of substitution (DS) of MA was calculated to be 7.5.

DOI: 10.1021/acsami.7b15832
ACS Appl. Mater. Interfaces 2018, 10, 3929−3937

HA-*g*-Lys-MTet was prepared by the carbodiimide reaction between MTet and HA-*g*-Lys-NH_2 (DS of Lys: 5.4) in the presence of *N*,*N*′-dicyclohexylcarbodiimide/4-dimethylaminopyridine (DCC/DMAP) (Scheme S2). Typically, DCC (754 mg, 3.66 mmol) was added into a stirred solution of MTet (420 mg, 1.43 mmol) in dimethyl sulfoxide (DMSO) (16.7 mL) under N_2. The reaction proceeded at room temperature for 12 h. Then, a solution of HA-Lys-NH_2 (500 mg, 143 μmol amino group) in anhydrous formamide (50 mL) and DMAP (298 mg, 1.43 mmol) were added, and the reaction solution was stirred for 48 h at 40 °C. The product was isolated by extensive dialysis (an MWCO of 3500) against DI water/DMSO (1:1, v/v) and then DI water followed by lyophilization. Yield: 63%. ^{1}H NMR (400 MHz, D_2O/DMSO-d_6, Figure S2, δ): MTet: 3.05, 6.75, 6.77, 7.86, and 7.88; Lys: 1.27, 1.51, 1.82, 2.79, 3.53 and 4.12; HA: 1.82, 3.05−3.63, and 4.30−4.38. The DS of MTet was calculated to be 5.4.

2.2. Fabrication of Fluorescent HMGs. HMGs were fabricated from HA-*g*-AMA and hyaluronic acid-*g*-lysine-4-(4-(dimethylamino)-phenyl-tetrazole)-benzoic acid by combining the microfluidics technique and photoclick chemistry. An aqueous solution of the two HA derivatives at an MTet/AMA molar ratio of 1 in phosphate buffer (PB, pH 7.4, 10 mM) with a total polymer concentration of 20 mg/mL as the core flow was hydrodynamically focused in a microchannel by the lateral mineral oil containing 5 wt % Span 80 to form microdroplets, followed by UV irradiation (302 nm, 18 mW/cm^2) for about 180 s. The collected microgels in the exit of the channel were purified by washing five times with PB to remove the mineral oil and surfactant. The size of the resultant microgels was determined using an inverted fluorescence microscope. By changing the flow rates of water and oil phases, HMGs with different sizes were easily obtained.

2.3. Loading and in Vitro Release of Proteins. The loading of proteins into microgels was easily accomplished by mixing of proteins (IgG and Herceptin) at a theoretical loading content of 30 wt % with an aqueous solution of HA derivatives (20 mg/mL) in PB as the core flow, followed by hydrodynamical focus in the microchannel by the lateral oil phase (5 wt % Span 80 in mineral oil) and subsequent UV irradiation. To calculate the protein-loading content and protein-loading efficiency, protein-loaded microgels (5 mg) were degraded with 600 U/mL HAase (500 μL) for 8 h, and the amounts of IgG and Herceptin were determined using an IgG human ELISA kit (Abcam, Massachusetts, USA) and a trastuzumab ELISA kit (Matriks Biotek Laboratories, Ankara, Turkey), respectively. Native proteins were used as controls.

For in vitro release study, 0.6 mL of the protein-loaded microgels (10 mg/mL) containing HAase was transferred to dialysis bags. The bags were then immersed in 25 mL of the release medium (PB, pH 7.4) under shaking at 100 rpm at 37 °C. At designated time intervals, 5 mL of the release medium was collected and replaced with a fresh medium. The amount of proteins such as Herceptin and IgG in the release medium was quantified using an ELISA kit. The results are presented as mean ± standard deviation. The secondary structure of the released proteins dissolved in PB (2 μg/mL) was analyzed at wavelengths of 200−250 nm by a circular dichroism (CD) spectrometer (J-1500, Jasco, Japan).

2.4. In Vivo Antitumor Efficacy Studies. When the tumor volume reached 100−120 mm^3, the tumor-bearing mice were randomly divided into six groups with six mice per group and treated with one dose of Herceptin-HMGs (30 mg Herceptin equiv/kg, sc), Herceptin-HMGs (15 mg Herceptin equiv/kg, sc), free Herceptin (30 mg Herceptin equiv/kg, sc), free Herceptin (30 mg Herceptin equiv/kg, iv), blank HMGs, or phosphate-buffered saline (PBS). Each sc treatment (200 μL) was divided into four injections and administered locally 5 mm away from the tumor block. Iv administration of free Herceptin was performed via the tail vein. The day of initiating the treatments was designated as day 0.

3. RESULTS AND DISCUSSION

3.1. Fabrication of Fluorescent HMGs. The aim of this work was to tailor-make biodegradable microgels that combine unique features of PLGA microparticles and hydrogels for the sustained and localized delivery of anticancer proteins. The microgels were fabricated from HA-*g*-AMA and HA-*g*-Lys-MTet via combining microfluidics and tetrazole−alkene photoclick chemistry. High specificity, fast reaction rate, and no requirement of catalysts make the photoclick reaction an ideal cross-linking strategy that causes little protein denaturation. Using the photoclick strategy, we have previously developed reduction-sensitive photoclick HA nanogels from HA−cystamine−methacrylate and HA−lysine−tetrazole and achieved efficient encapsulation and intracellular delivery of therapeutic proteins.[29,34] Here, HA-*g*-AMA was prepared by conjugating AMA onto HA in the presence of DMTMM (Scheme S1). ^{1}H NMR displayed, besides the signals attributable to HA (1.96, 3.28−3.84, and 4.41−4.47), also resonances due to the AMA protons at δ 6.08, 5.68, and 1.86 (Figure S1). The DS of AMA, defined as the number of AMA units per 100 sugar residues of an HA polymer, was determined to be 7.5 by comparing the integrals of the signals at δ 6.08 and 5.68 (vinyl protons in AMA) with those of the signals at 4.41 and 4.47 (anomeric proton in HA). HA-*g*-Lys-MTet was obtained by conjugating MTet onto HA-Lys-NH_2 by carbodiimide chemistry (Scheme S2). ^{1}H NMR of HA-*g*-Lys-MTet showed clear signals at δ 6.75, 6.77, 7.86, and 7.88 attributable to the phenyl protons of MTet (Figure S2). The comparison of the signals at δ 6.75−6.77 (phenyl protons of MTet) and δ 4.30−3.38 (anomeric protons in HA) revealed a DS of 5.4, indicating a quantitative conjugation of MTet.

Microdroplets with defined sizes were generated swiftly in a microfluidics chip from an aqueous solution of HA-*g*-AMA/HA-*g*-Lys-MTet mixture and mineral oil containing 5 wt % Span 80 (Video 1). The microscopy images demonstrated that thus formed microdroplets had uniform sizes and spherical morphologies (Figure 1B,C), in which microdroplets with a diameter of 55 μm were obtained when the water phase flow rate and oil phase flow rate were 5 and 1 μL/mL, respectively. The microdroplets following UV irradiation formed robust microgels, which displayed a slightly decreased size and monodispersity (Figure 1B,C). In sharp contrast with the traditional miniemulsion method that often generates microgels with a broad size distribution,[35] the microfluidic strategy has been reported to afford unprecedented control over the size and shape of microparticles.[36,37] Moreover, the microfluidic technique allows both microdroplet formation and cross-linking to take place in the microfluidic chip, greatly simplifying the microgel preparation and increasing the reproducibility. The tetrazole−alkene photoclick reaction not only provides microgels with strong fluorescence with an emission wavelength of 480 nm (excitation at 365 nm) (Figure S4) for their tracking in cells and tumor tissues[29,38] but also facilitates spatiotemporal control over cross-linking. Notably, the size of microgels could be easily controlled by adjusting the flow rates of the water and oil phases. For example, the diameter of microgels decreased from 50 to 25 μm with the flow rate of the oil phase increasing from 5 to 10 μL/mL (Figure 1B,C). HMGs with a diameter of 50 μm were employed for the following in vitro and in vivo experiments. Injectable hydrogels with high water content and excellent biocompatibility have been extensively explored for protein delivery.[39−41] However, most injectable hydrogels cannot be easily translated into clinical practice because of the difficulty in balancing gelation time, injectability, and gel strength.[42−44]

3.2. Enzymatic Degradation of Microgels. The in vitro degradation of HMGs was tracked by fluorescence microscopy.

DOI: 10.1021/acsami.7b15832
ACS Appl. Mater. Interfaces 2018, 10, 3929−3937

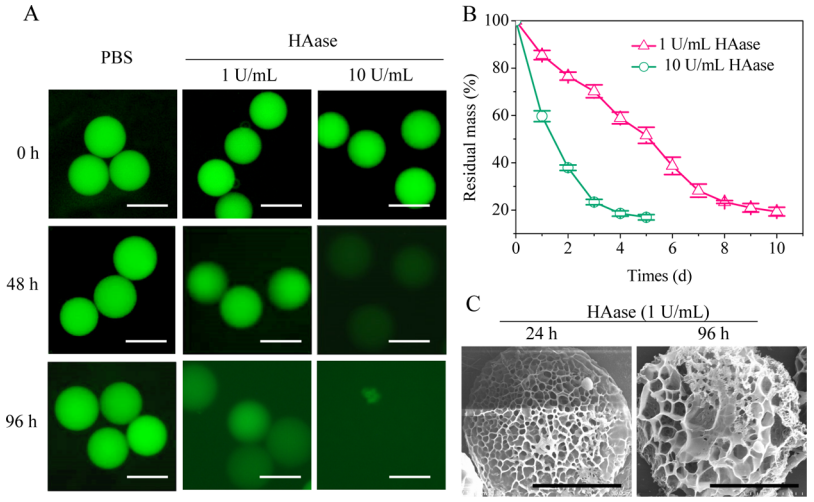

Figure 2. Enzymatic degradation of HMGs in the presence of 1 or 10 U/mL HAase at 37 °C. (A) Changes of fluorescence images over time. Scale bars, 50 μm; (B) weight loss over time. Data are presented as mean ± SD (n = 3); (C) SEM images of HMGs treated with 1 U/mL HAase for 24 or 96 h. Scale bars, 25 μm.

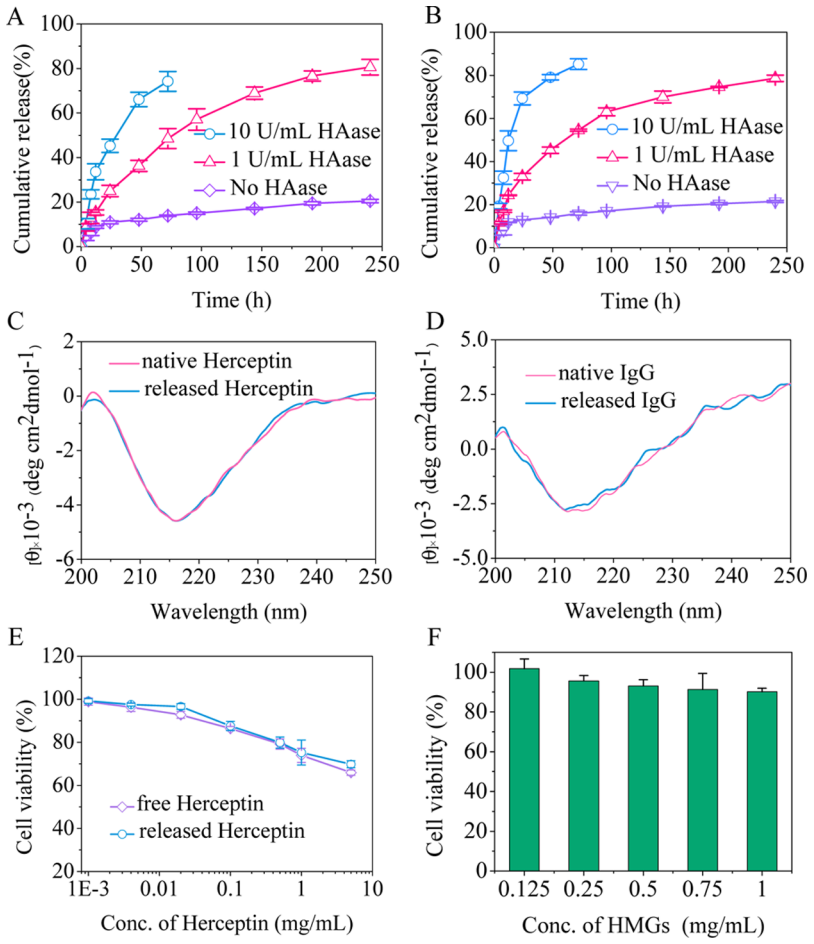

Figure 3. (A) HAase-dependent release of Herceptin from HMGs; (B) HAase-dependant release of IgG from HMGs; (C) CD spectra of free and released Herceptin; (D) CD spectra of free and released IgG; (E) MTT assays of released or free Herceptin in SKOV-3 cells following 48 h of incubation; and (F) MTT assays of blank HMGs in SKOV-3 cells following 48 h of incubation. Data are presented as mean ± SD (n = 4).

The results displayed negligible changes of the size and fluorescence intensity for the microgels incubated in PB for over 96 h (Figure 2A), indicating that the HMGs are stable under physiological conditions. In contrast, physically cross-linked HA microsystems showed generally a low stability.[45,46]

The HMGs following the treatment of HAase displayed a slightly increased size and largely diminished fluorescence, in which the HMGs treated with 10 U/mL HAase for 48 h revealed negligible fluorescence (Figure 2A). Figure 2B reveals that ca. 80 wt % of HMGs was degraded following a 10 h

DOI: 10.1021/acsami.7b15832
ACS Appl. Mater. Interfaces 2018, 10, 3929−3937

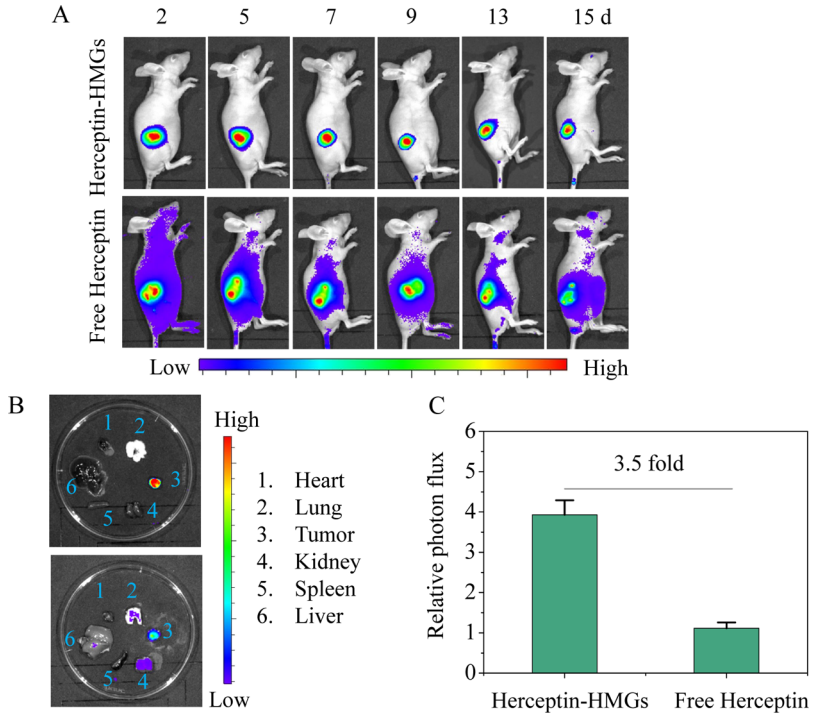

Figure 4. (A) In vivo fluorescence images of SKOV-3 tumor-bearing nude mice at different times, following sc injection of Cy5-labeled Herceptin-HMGs or Cy5-labeled Herceptin; (B) ex vivo fluorescence images of the major organs and tumor excised from SKOV-3 tumor-bearing nude mice, following 15 days of treatment with Cy5-labeled Herceptin-HMGs (top) or Cy5-labeled Herceptin (bottom); and (C) semiquantified average fluorescence levels of tumors, following 15 days of treatment. Data are presented as mean ± SD (n = 3).

incubation with 1 U/mL HAase or 5 h with 10 U/mL HAase. Scanning electron microscopy (SEM) images demonstrated that the HMGs following the treatment with HAase had a rough surface and large pores (Figure 2C). HAase is known to exist in the human body, and especially in tumor tissues.[31,32] Hence, these enzymatically degradable HMGs could be a promising platform to achieve a sustained and localized release of therapeutic agents in the tumor.

3.3. HAase-Dependent Protein Release and Cytotoxicity. Proteins could be easily loaded into HMGs, in which loading efficiencies of 94.7 and 90.8% were achieved for Herceptin and IgG, respectively, at a theoretical loading content of 30 wt %. The high protein-loading capacity could be attributed to the high stability of HMGs and the strong electrostatic interactions between positively charged proteins and negatively charged microgels. In vitro release experiments revealed less than 25% Herceptin release from HMGs in 10 days in PB, whereas over 80% of Herceptin was released in 10 days under the 1 U/mL HAase condition (Figure 3A). In the presence of 10 U/mL HAase, the protein release rate was further accelerated in which ca. 80% of Herceptin was released in 3 days. IgG displayed release profiles similar to those of Herceptin, in which 78.6 and 85.2% of IgG were released from HMGs in 10 days under 1 U/mL HAase and 3 days under 10 U/mL HAase, respectively (Figure 3B). Notably, CD measurements revealed that the released proteins including Herceptin and IgG had a secondary structure similar to those of native proteins (Figure 3C,D), indicating that this microgel fabrication procedure is mild and has no detrimental effect on the secondary structure of the encapsulated proteins.

The in vitro antitumor activity of released Herceptin was evaluated by MTT assays in SKOV-3 cells. The results showed that the cells treated with native Herceptin and released Herceptin had comparable cell viabilities at Herceptin concentrations of 0.001−5 mg/mL (Figure 3E), indicating that the released proteins from microgels retained a similar antitumor activity to native proteins. Importantly, blank HMGs displayed over 90% cell viability against SKOV-3 cells, even at a concentration up to 1 mg/mL (Figure 3F), signifying their excellent biocompatibility. To rule out the possible effect of HAase, SKOV-3 cells were treated with HAase at concentrations of 0.12−600 U/mL at 37 °C for 48 h to assess its cytotoxicity. The results demonstrated that cells following treatment with 600 U/mL HAase revealed a 100% cell viability (Figure S5). All results pointed out that Herceptin released from microgels maintained a high potency toward cancer cells.

3.4. Biodistribution of Herceptin-Loaded HMGs. A near-infrared Cy5 dye was labeled on Herceptin to facilitate the observation of its biodistribution in SKOV-3 tumor-bearing nude mice by noninvasive fluorescence imaging. Interestingly, a strong Cy5 fluorescence was observed in the tumor sites of mice subcutaneously injected with the Cy5-labeled Herceptin-loaded HMGs from 2 to 15 days (Figure 4A), indicating long tumoral retention of HMGs. In comparison, mice treated with free Herceptin (sc) displayed an obviously decreased Cy5 fluorescence intensity in the tumor over time (Figure 4A), which is matched with the short half-life (~1 week) of Herceptin.[47] Furthermore, the Cy5 fluorescence of free Herceptin distributed throughout the whole body. The ex vivo fluorescence images clearly showed that the Herceptin-HMG group had a much higher tumoral accumulation of Cy5-Herceptin than the free Cy5-Herceptin group at 15 days post injection (Figure 4B). Moreover, the mice treated with Herceptin-HMGs displayed a relatively lower Cy5 fluorescence in healthy organs such as kidneys, lungs, and liver than those treated with free Herceptin. Semiquantitative analysis revealed

DOI: 10.1021/acsami.7b15832
ACS Appl. Mater. Interfaces 2018, 10, 3929−3937

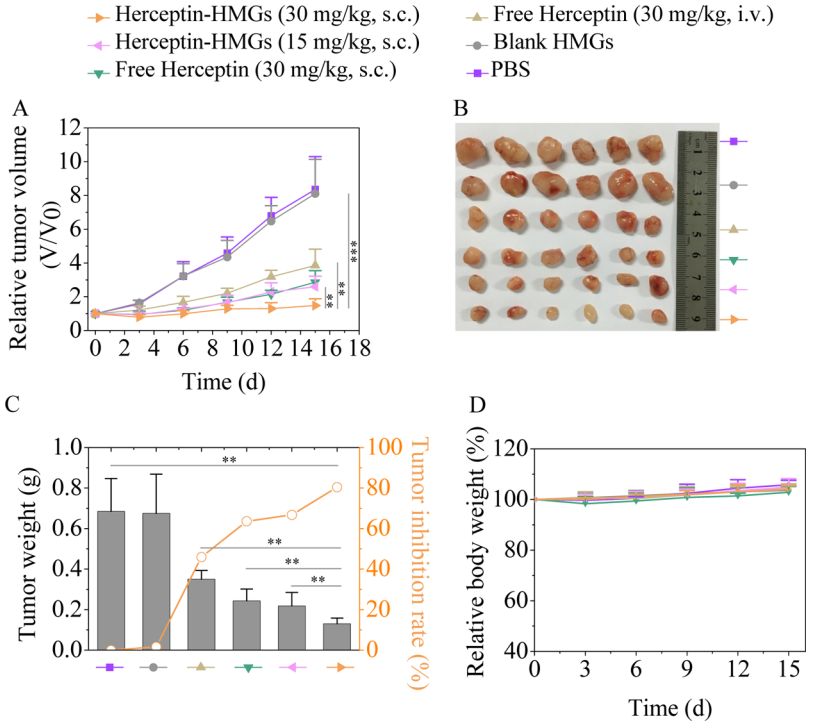

Figure 5. Treatment of SKOV-3 ovarian tumor-bearing nude mice by sc injection of Herceptin-loaded HMGs at 15 or 30 mg Herceptin equiv/kg. Sc or systemic injection of 30 mg/kg free Herceptin and sc injection of blank HMGs or PBS were used as controls. (A) Changes of mice tumor volume over time; (B) photographs of the tumor blocks collected on day 15 from different treatment groups; (C) tumor weight and TIR on day 15; and (D) body weight changes in 15 days. Data are presented as mean ± SD (n = 6).

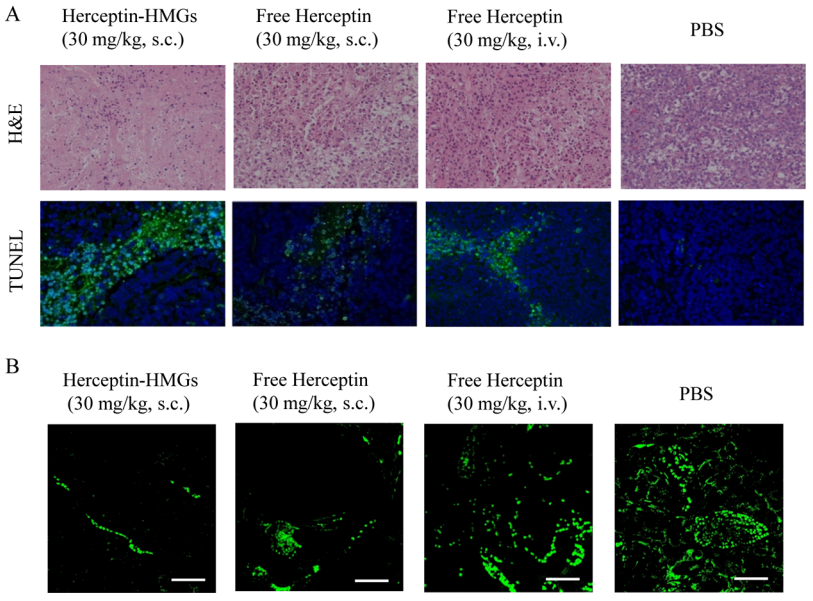

Figure 6. (A) H&E staining and TUNEL staining of tumor sections following 15 days of treatment (40×). (B) Representative fluorescence images of blood vessels in tumor sections following 15 days of treatment. Scale bars, 50 μm.

that the Herceptin-HMG group had a 3.5-fold higher fluorescence intensity in the tumor site than the free Herceptin group on day 15 (Figure 4C). These results signify that Herceptin-HMGs are able to achieve localized and sustained release of therapeutic proteins in the tumor while largely reducing the protein diffusion to healthy organs.

3.5. In Vivo Therapeutic Efficacy. Ovarian cancer is one of the most malignant tumors that cause a high mortality in women.[48,49] The therapeutic performance of Herceptin-HMGs was evaluated using SKOV-3 ovarian tumor-bearing nude mice. It should be noted that HMGs with a size of 50 μm were designed for the sustained and localized delivery of proteins, and thus Herceptin-HMGs were administered via sc injection instead of iv administration. The results demonstrated that tumor growth was efficiently suppressed by sc administration of Herceptin-HMGs at a dose of 30 mg Herceptin equiv/kg, which was significantly more effective than free Herceptin administered via either sc or iv injection at the same protein

DOI: 10.1021/acsami.7b15832
ACS Appl. Mater. Interfaces 2018, 10, 3929−3937

dose (Figure 5A). Notably, Herceptin-HMGs at a lower dosage of 15 mg of Herceptin/kg caused a tumor inhibition similar to that by free Herceptin at 30 mg/kg. The photographs of the tumor blocks isolated on day 15 verified that Herceptin-HMGs at a dose of 30 mg Herceptin equiv/kg had the smallest tumor volumes (Figure 5B). Further analyses on tumor weights displayed that Herceptin-HMGs at a dose of 30 mg Herceptin equiv/kg had an improved tumor inhibition rate (TIR) of 80% (Figure 5C), which was significantly higher than that of free Herceptin via either iv (46%) or sc (64%) administration. Herceptin-HMGs caused little body weight change during the whole treatment period (Figure 5D), indicating that Herceptin-HMGs had negligible systemic toxicity. Yang et al. reported that injectable polycarbonate hydrogels achieved a sustained release of Herceptin, giving better therapeutic efficacy in BT-474 breast tumor-bearing mice than free Herceptin.[8]

H&E staining revealed that Herceptin-HMGs at a dose of 30 mg Herceptin equiv/kg induced widespread necrosis of SKOV-3 tumor cells, which was obviously more effective than free Herceptin (Figure 6A). TUNEL assays further showed that Herceptin-HMGs at a dose of 30 mg Herceptin equiv/kg caused significantly more apoptosis than free Herceptin (Figure 6A). In consistence with the results of tumor growth suppression, Herceptin-HMGs at a lower dosage of 15 mg of Herceptin/kg displayed less necrosis and apoptosis (Figure S6). Figure S7 shows that Herceptin-HMGs at both high and low dosages caused little damage to healthy organs such as liver, heart, and kidneys, confirming that they have low toxicity. Notably, both free Herceptin and Herceptin-HMG groups showed significantly decreased blood vessels in tumors in comparison with the PBS group, whereas mice treated with Herceptin-HMGs at 30 mg Herceptin equiv/kg revealed further fewer blood vessels in tumors (Figures 6B and S8), corroborating that Herceptin can effectively inhibit tumor angiogenesis.[50,51]

4. CONCLUSIONS

We have demonstrated that fluorescent HMGs can be tailor-made by combining microfluidics and tetrazole−alkene photo-click chemistry to achieve sustained and localized delivery of Herceptin to ovarian cancer in vivo. Notably, HMGs display a precisely controlled size, high colloidal stability, enzymatic degradability, high protein-loading capacity, and sustained and HAase-dependent protein-release behavior. The released proteins maintain their secondary structure and antitumor activity. Herceptin-loaded HMGs display significantly higher tumoral accumulation of Herceptin and less diffusion to healthy organs in comparison with the free protein. The therapeutic studies corroborate that Herceptin-HMGs at a dose of 30 mg Herceptin equiv/kg completely suppress tumor growth in SKOV-3 human ovarian carcinoma-bearing mice. This represents the first proof-of-concept study on the sustained and localized delivery of therapeutic proteins using microgels for cancer treatment.

■ ASSOCIATED CONTENT

Supporting Information

The Supporting Information is available free of charge on the ACS Publications website at DOI: 10.1021/acsami.7b15832.

Materials, characterization, synthesis of HA-*g*-AMA and HA-*g*-Lys-MTet, degradation of HMGs, MTT assays, biodistribution, histological and immunofluorescence analyses, and additional schemes and figures (PDF)

Microdroplets with defined sizes generated swiftly in a microfluidics chip from an aqueous solution of HA-*g*-AMA/HA-*g*-Lys-MTet mixture and mineral oil containing 5 wt % Span 80 (AVI)

■ AUTHOR INFORMATION

Corresponding Authors

*E-mail: cdeng@suda.edu.cn (C.D.).
*E-mail: zyzhong@suda.edu.cn (Z.Z.).

ORCID

Chao Deng: 0000-0001-7697-9874
Zhiyuan Zhong: 0000-0003-4175-4741

Notes

The authors declare no competing financial interest.

■ ACKNOWLEDGMENTS

This work was supported by the National Natural Science Foundation of China (NSFC 51773145, 51473110, 51403147, and 51633005) and a Project Funded by the Priority Academic Program Development of Jiangsu Higher Education Institutions.

■ REFERENCES

(1) Scott, A. M.; Wolchok, J. D.; Old, L. J. Antibody Therapy of Cancer. *Nat. Rev. Cancer* **2012**, *12*, 278−287.

(2) Chari, R. V. J.; Miller, M. L.; Widdison, W. C. Antibody-Drug Conjugates: An Emerging Concept in Cancer Therapy. *Angew. Chem., Int. Ed.* **2014**, *53*, 3796−3827.

(3) Amiri-Kordestani, L.; Blumenthal, G. M.; Xu, Q. C.; Zhang, L.; Tang, S. W.; Ha, L.; Weinberg, W. C.; Chi, B.; Candau-Chacon, R.; Hughes, P.; Russell, A. M.; Miksinski, S. P.; Chen, X. H.; McGuinn, W. D.; Palmby, T.; Schrieber, S. J.; Liu, Q.; Wang, J.; Song, P.; Mehrotra, N.; Skarupa, L.; Clouse, K.; Al-Hakim, A.; Sridhara, R.; Ibrahim, A.; Justice, R.; Pazdur, R.; Cortazar, P. FDA Approval: Ado-Trastuzumab Emtansine for the Treatment of Patients with HER2-Positive Metastatic Breast Cancer. *Clin. Cancer Res.* **2014**, *20*, 4436−4441.

(4) Sapiezynski, J.; Taratula, O.; Rodriguez-Rodriguez, L.; Minko, T. Precision Targeted Therapy of Ovarian Cancer. *J. Controlled Release* **2016**, *243*, 250−268.

(5) Magnifico, A.; Albano, L.; Campaner, S.; Delia, D.; Castiglioni, F.; Gasparini, P.; Sozzi, G.; Fontanella, E.; Menard, S.; Tagliabue, E. Tumor-Initiating Cells of HER2-Positive Carcinoma Cell Lines Express the Highest Oncoprotein Levels and Are Sensitive to Trastuzumab. *Clin. Cancer Res.* **2009**, *15*, 2010−2021.

(6) Liu, Y. J.; Shen, D.; Yin, X.; Gavine, P.; Zhang, T.; Su, X.; Zhan, P.; Xu, Y.; Lv, J.; Qian, J.; Liu, C.; Sun, Y.; Qian, Z.; Zhang, J.; Gu, Y.; Ni, X. HER2, MET and FGFR2 Oncogenic Driver Alterations Define Distinct Molecular Segments for Targeted Therapies in Gastric Carcinoma. *Br. J. Cancer* **2014**, *110*, 1169−1178.

(7) Pritchard, K. I. Optimizing the Delivery of Targeted Research: An Opportunity for Comparative Effectiveness Research. *J. Clin. Oncol.* **2010**, *28*, 1089−1091.

(8) Lee, A. L. Z.; Ng, V. W. L.; Gao, S.; Hedrick, J. L.; Yang, Y. Y. Injectable Hydrogels from Triblock Copolymers of Vitamin E-Functionalized Polycarbonate and Poly(Ethylene Glycol) for Subcutaneous Delivery of Antibodies for Cancer Therapy. *Adv. Funct. Mater.* **2014**, *24*, 1538−1550.

(9) Vermonden, T.; Censi, R.; Hennink, W. E. Hydrogels for Protein Delivery. *Chem. Rev.* **2012**, *112*, 2853−2888.

(10) Gause, K. T.; Wheatley, A. K.; Cui, J.; Yan, Y.; Kent, S. J.; Caruso, F. Immunological Principles Guiding the Rational Design of Particles for Vaccine Delivery. *ACS Nano* **2017**, *11*, 54−68.

DOI: 10.1021/acsami.7b15832
ACS Appl. Mater. Interfaces 2018, 10, 3929−3937

(11) Yu, M.; Wu, J.; Shi, J.; Farokhzad, O. C. Nanotechnology for Protein Delivery: Overview and Perspectives. *J. Controlled Release* **2016**, *240*, 24−37.
(12) Lu, Y.; Sun, W.; Gu, Z. Stimuli-Responsive Nanomaterials for Therapeutic Protein Delivery. *J. Controlled Release* **2014**, *194*, 1−19.
(13) Jiang, Y.; Chen, J.; Deng, C.; Suuronen, E. J.; Zhong, Z. Click Hydrogels, Microgels and Nanogels: Emerging Platforms for Drug Delivery and Tissue Engineering. *Biomaterials* **2014**, *35*, 4969−4985.
(14) Maina, J. W.; Richardson, J. J.; Chandrawati, R.; Kempe, K.; van Koeverden, M. P.; Caruso, F. Capsosomes as Long-Term Delivery Vehicles for Protein Therapeutics. *Langmuir* **2015**, *31*, 7776−7781.
(15) Mundargi, R. C.; Babu, V. R.; Rangaswamy, V.; Patel, P.; Aminabhavi, T. M. Nano/Micro Technologies for Delivering Macromolecular Therapeutics Using Poly(D,L-Lactide-co-Glycolide) and Its Derivatives. *J. Controlled Release* **2008**, *125*, 193−209.
(16) Rahimian, S.; Fransen, M. F.; Kleinovink, J. W.; Amidi, M.; Ossendorp, F.; Hennink, W. E. Polymeric Microparticles for Sustained and Local Delivery of AntiCD40 and AntiCTLA-4 in Immunotherapy of Cancer. *Biomaterials* **2015**, *61*, 33−40.
(17) Peres, C.; Matos, A. I.; Conniot, J.; Sainz, V.; Zupančič, E.; Silva, J. M.; Graça, L.; Gaspar, R. S.; Préat, V.; Florindo, H. F. Poly(Lactic Acid)-Based Particulate Systems Are Promising Tools for Immune Modulation. *Acta Biomater.* **2017**, *48*, 41−57.
(18) Danhier, F.; Ansorena, E.; Silva, J. M.; Coco, R.; Le Breton, A.; Préat, V. PLGA-Based Nanoparticles: An Overview of Biomedical Applications. *J. Controlled Release* **2012**, *161*, 505−522.
(19) Loh, X. J. Supramolecular Host−Guest Polymeric Materials for Biomedical Applications. *Mater. Horiz.* **2014**, *1*, 185−195.
(20) Fettis, M. M.; Wei, Y.; Restuccia, A.; Kurian, J. J.; Wallet, S. M.; Hudalla, G. A. Microgels with Tunable Affinity-Controlled Protein Release Via Desolvation of Self-Assembled Peptide Nanofibers. *J. Mater. Chem. B* **2016**, *4*, 3054−3064.
(21) Kim, P.-H.; Yim, H.-G.; Choi, Y.-J.; Kang, B.-J.; Kim, J.; Kwon, S.-M.; Kim, B.-S.; Hwang, N. S.; Cho, J.-Y. Injectable Multifunctional Microgel Encapsulating Outgrowth Endothelial Cells and Growth Factors for Enhanced Neovascularization. *J. Controlled Release* **2014**, *187*, 1−13.
(22) Zykwinska, A.; Marquis, M.; Sinquin, C.; Cuenot, S.; Colliec-Jouault, S. Assembly of HE800 Exopolysaccharide Produced by a Deep-Sea Hydrothermal Bacterium into Microgels for Protein Delivery Applications. *Carbohydr. Polym.* **2016**, *142*, 213−221.
(23) Rios, J. L.; Lu, G.; Seo, N. E.; Lambert, T.; Putnam, D. Prolonged Release of Bioactive Model Proteins from Anionic Microgels Fabricated with a New Microemulsion Approach. *Pharm. Res.* **2016**, *33*, 879−892.
(24) Gu, Z.; Dang, T. T.; Ma, M.; Tang, B. C.; Cheng, H.; Jiang, S.; Dong, Y.; Zhang, Y.; Anderson, D. G. Glucose-Responsive Microgels Integrated with Enzyme Nanocapsules for Closed-Loop Insulin Delivery. *ACS Nano* **2013**, *7*, 6758−6766.
(25) Wu, Y.; Hu, H.; Hu, J.; Liu, S. Glucose-Regulated Insulin Release from Acid-Disintegrable Microgels Covalently Immobilized with Glucose Oxidase and Catalase. *Macromol. Rapid Commun.* **2012**, *33*, 1852−1860.
(26) Foster, G. A.; Headen, D. M.; González-García, C.; Salmerón-Sánchez, M.; Shirwan, H.; García, A. J. Protease-Degradable Microgels for Protein Delivery for Vascularization. *Biomaterials* **2017**, *113*, 170−175.
(27) Zhao, X.; Liu, S.; Yildirimer, L.; Zhao, H.; Ding, R.; Wang, H.; Cui, W.; Weitz, D. Injectable Stem Cell-Laden Photocrosslinkable Microspheres Fabricated Using Microfluidics for Rapid Generation of Osteogenic Tissue Constructs. *Adv. Funct. Mater.* **2016**, *26*, 2809−2819.
(28) Song, W.; Wang, Y.; Qu, J.; Madden, M. M.; Lin, Q. A Photoinducible 1,3-Dipolar Cycloaddition Reaction for Rapid, Selective Modification of Tetrazole-Containing Proteins. *Angew. Chem., Int. Ed.* **2008**, *47*, 2832−2835.
(29) Chen, J.; Zou, Y.; Deng, C.; Meng, F.; Zhang, J.; Zhong, Z. Multifunctional Click Hyaluronic Acid Nanogels for Targeted Protein Delivery and Effective Cancer Treatment in Vivo. *Chem. Mater.* **2016**, *28*, 8792−8799.
(30) Oh, E. J.; Park, K.; Kim, K. S.; Kim, J.; Yang, J.-A.; Kong, J.-H.; Lee, M. Y.; Hoffman, A. S.; Hahn, S. K. Target Specific and Long-Acting Delivery of Protein, Peptide, and Nucleotide Therapeutics Using Hyaluronic Acid Derivatives. *J. Controlled Release* **2010**, *141*, 2−12.
(31) Stern, R.; Jedrzejas, M. J. Hyaluronidases: Their Genomics, Structures, and Mechanisms of Action. *Chem. Rev.* **2006**, *106*, 818−839.
(32) Jiang, T.; Mo, R.; Bellotti, A.; Zhou, J.; Gu, Z. Gel-Liposome-Mediated Co-Delivery of Anticancer Membrane-Associated Proteins and Small-Molecule Drugs for Enhanced Therapeutic Efficacy. *Adv. Funct. Mater.* **2014**, *24*, 2295−2304.
(33) Fan, Y.; Deng, C.; Cheng, R.; Meng, F.; Zhong, Z. In Situ Forming Hydrogels Via Catalyst-Free and Bioorthogonal "Tetrazole−Alkene" Photo-Click Chemistry. *Biomacromolecules* **2013**, *14*, 2814−2821.
(34) Chen, J.; Ouyang, J.; Chen, Q.; Deng, C.; Meng, F.; Zhang, J.; Cheng, R.; Lan, Q.; Zhong, Z. EGFR and CD44 Dual-Targeted Multifunctional Hyaluronic Acid Nanogels Boost Protein Delivery to Ovarian and Breast Cancers in Vitro and in Vivo. *ACS Appl. Mater. Interfaces* **2017**, *9*, 24140−24147.
(35) Jiang, Z.; Xia, B.; McBride, R.; Oakey, J. A Microfluidic-Based Cell Encapsulation Platform to Achieve High Long-Term Cell Viability in Photopolymerized PEGNB Hydrogel Microspheres. *J. Mater. Chem. B* **2017**, *5*, 173−180.
(36) Wang, W.; Zhang, M.-J.; Chu, L.-Y. Functional Polymeric Microparticles Engineered from Controllable Microfluidic Emulsions. *Acc. Chem. Res.* **2014**, *47*, 373−384.
(37) Steinhilber, D.; Rossow, T.; Wedepohl, S.; Paulus, F.; Seiffert, S.; Haag, R. A Microgel Construction Kit for Bioorthogonal Encapsulation and pH-Controlled Release of Living Cells. *Angew. Chem., Int. Ed.* **2013**, *52*, 13538−13543.
(38) Li, S.; Zhang, J.; Deng, C.; Meng, F.; Yu, L.; Zhong, Z. Redox-Sensitive and Intrinsically Fluorescent Photoclick Hyaluronic Acid Nanogels for Traceable and Targeted Delivery of Cytochrome C to Breast Tumor in Mice. *ACS Appl. Mater. Interfaces* **2016**, *8*, 21155−21162.
(39) Lee, A. L. Z.; Ng, V. W. L.; Gao, S.; Hedrick, J. L.; Yang, Y. Y. Injectable Biodegradable Hydrogels from Vitamin D-Functionalized Polycarbonates for the Delivery of Avastin with Enhanced Therapeutic Efficiency against Metastatic Colorectal Cancer. *Biomacromolecules* **2015**, *16*, 465−475.
(40) Wu, X.; He, C.; Wu, Y.; Chen, X. Synergistic Therapeutic Effects of Schiff's Base Cross-Linked Injectable Hydrogels for Local Co-Delivery of Metformin and 5-Fluorouracil in a Mouse Colon Carcinoma Model. *Biomaterials* **2016**, *75*, 148−162.
(41) Chen, Y.; Luan, J.; Shen, W.; Lei, K.; Yu, L.; Ding, J. Injectable and Thermosensitive Hydrogel Containing Liraglutide as a Long-Acting Antidiabetic System. *ACS Appl. Mater. Interfaces* **2016**, *8*, 30703−30713.
(42) Lee, F.; Chung, J. E.; Kurisawa, M. An Injectable Hyaluronic Acid−Tyramine Hydrogel System for Protein Delivery. *J. Controlled Release* **2009**, *134*, 186−193.
(43) Patenaude, M.; Campbell, S.; Kinio, D.; Hoare, T. Tuning Gelation Time and Morphology of Injectable Hydrogels Using Ketone−Hydrazide Cross-Linking. *Biomacromolecules* **2014**, *15*, 781−790.
(44) Kim, I.; Choi, J. S.; Lee, S.; Byeon, H. J.; Lee, E. S.; Shin, B. S.; Choi, H.-G.; Lee, K. C.; Youn, Y. S. In Situ Facile-Forming PEG Cross-Linked Albumin Hydrogels Loaded with an Apoptotic Trail Protein. *J. Controlled Release* **2015**, *214*, 30−39.
(45) Lim, S. T.; Martin, G. P.; Berry, D. J.; Brown, M. B. Preparation and Evaluation of the in Vitro Drug Release Properties and Mucoadhesion of Novel Microspheres of Hyaluronic Acid and Chitosan. *J. Controlled Release* **2000**, *66*, 281−292.
(46) Kim, S. J.; Hahn, S. K.; Kim, M. J.; Kim, D. H.; Lee, Y. P. Development of a Novel Sustained Release Formulation of

DOI: 10.1021/acsami.7b15832
ACS Appl. Mater. Interfaces 2018, 10, 3929−3937

Recombinant Human Growth Hormone Using Sodium Hyaluronate Microparticles. *J. Controlled Release* **2005**, *104*, 323−335.
(47) Harries, M.; Smith, I. The Development and Clinical Use of Trastuzumab (Herceptin). *Endocr.-Relat. Cancer* **2002**, *9*, 75−85.
(48) Ferlay, J.; Soerjomataram, I.; Dikshit, R.; Eser, S.; Mathers, C.; Rebelo, M.; Parkin, D. M.; Forman, D.; Bray, F. Cancer Incidence and Mortality Worldwide: Sources, Methods and Major Patterns in Globocan 2012. *Int. J. Cancer* **2015**, *136*, E359−E386.
(49) Rao, D. A.; Mishra, G.; Doddapaneni, B. S.; Kyryachenko, S.; Wierzbicki, I. H.; Ngyuen, D. X.; Shah, V.; Al Fatease, A. M.; Alany, R. G.; Alani, A. W. G. Combinatorial Polymeric Conjugated Micelles with Dual Cytotoxic and Antiangiogenic Effects for the Treatment of Ovarian Cancer. *Chem. Mater.* **2016**, *28*, 6068−6079.
(50) Izumi, Y.; Xu, L.; di Tomaso, E.; Fukumura, D.; Jain, R. K. Tumor Biology: Herceptin Acts as an Anti-Angiogenic Cocktail. *Nature* **2002**, *416*, 279−280.
(51) McDonald, D. M.; Baluk, P. Significance of Blood Vessel Leakiness in Cancer. *Cancer Res.* **2002**, *62*, 5381−5385.

DOI: 10.1021/acsami.7b15832
ACS Appl. Mater. Interfaces 2018, 10, 3929−3937